Delft University of Technology

ROBUST CONTROL
SC42145

Assignment: SISO Analysis and Control Design

Authors:
Luuk Bartels (4881923)
Pieter van Bentum (4694732)

December 15, 2022

Contents

1 SISO Analysis and Control Design

1.1

By subtracting the SISO system from FWT we get the bode plots shown in figures 1. In the pole-zero map we see that we have two zeros in the RHP. We cannot cancel these zeros with poles, because then we would have poles in the RHP letting the system become unstable. We have a pair of complex conjugate RHP-zeros $z = 0.0038 \pm 0.2i$ which limits our bandwidth frequency by [2][p. 186]:

$$\omega_B^* < -\frac{x}{M} + \sqrt{x^2 + y^2\left(1 - \frac{1}{M^2}\right)} \tag{1}$$

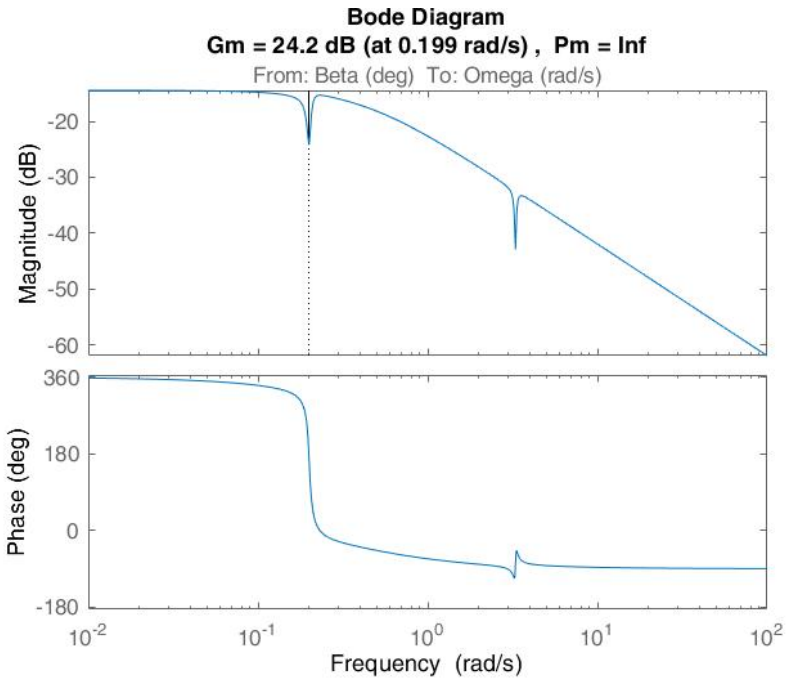

Figure 1: The bode plots of the SISO system.

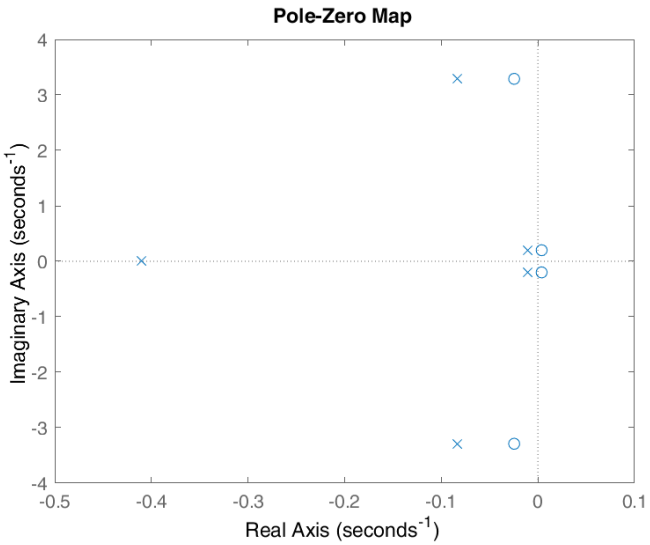

Figure 2: The pole zero map of the SISO system.

In the bode diagram we see two anti-resonance points which can limit the bandwidth. Because the anti-resonance

points are a valley there is a chance that the -3dB line gets crossed earlier than without the anti-resonance valley and so the bandwidth will be lower than without the anti-resonance valley and therefore limits our design.

1.2

The three requirements for this assignment are listed down below.

1. Small settling-time
2. Overshoot $<1\%$
3. No steady state error

Formulating these requirements in the frequency domain results in the following.

1. In general a larger crossover frequency leads to a faster rise time. Where a faster rise time attributes to a smaller settling-time (if there is not much oscillation). As with a higher crossover frequency you better preserve the high frequencies which make the system react quicker. However, it is important to also make sure the lower frequencies are not too much amplified by the transfer function. So to have a small settling time one need to find the optimum trade-off between these two aspects.
2. Overshoot is related to the phase margin. A higher phase margin means a lower overshoot. So in our frequency domain we are looking for a high enough phase margin in order to achieve an overshoot of $<1\%$. The formula for the overshoot is given as [1][p. 160]:

$$Overshoot = 100 \exp\left(\frac{-\zeta\pi}{\sqrt{1-\zeta^2}}\right) \tag{2}$$

   For this assignment we want an overshoot of less then 1% and if we fill this in we get a damping ratio of 0.826. The damping ratio is related to the phase margin in the frequency domain via this equation [1][p. 397]:

$$\phi_{Margin} = \tan^{-1} \frac{2\zeta}{\sqrt{-2\zeta^2 + \sqrt{1+4\zeta^4}}} \tag{3}$$

   If we fill in the damping ration we found earlier we get a phase margin of around 70.9 degree. So we need a phase margin of at least 70.9 degree to get a overshoot of less then 1%.
3. We reduce the steady-state errors by shaping the sensitivity function. In which it is important that the low frequencies are attenuated, as otherwise you would see the effect of the disturbance back in the steady-state. When the disturbance is heavily attenuated it is still important to have a good reference tracking to reduce the error in steady-state. A complementary sensitivity of around 1 for the low frequencies makes that happen.

1.3

The RHP zeros cause a 180 degree phase shift in the bode diagram and because we have two poles close to the origin there will be another 180 degree phase shift (see figure 2 for the pole-zero map). This phase shift can be seen in figure 1. Because of this phase shift the phase will go through -180 degree (we can shift the phase 360 degree in the bode diagram) at this frequency and thus our bandwidth cannot be greater than this frequency. If we add a proportional gain in our controller the bode magnitude diagram will shift up and if the gain is too high the cross-over frequency will be greater than the bandwidth and thus the phase margin will be negative which gives an unstable system. If we look at the locus plot of the system we can also see the problem of adding a proportional gain in the controller. In figure 3 we see that the poles close to the origin will move to the RHP zeros which will happen with a very small proportional gain, making the system unstable. As one can see in figure 3 for already a small gain of 3.26 the poles start moving to the RHP. So we chose to not have a K_p in our controller.

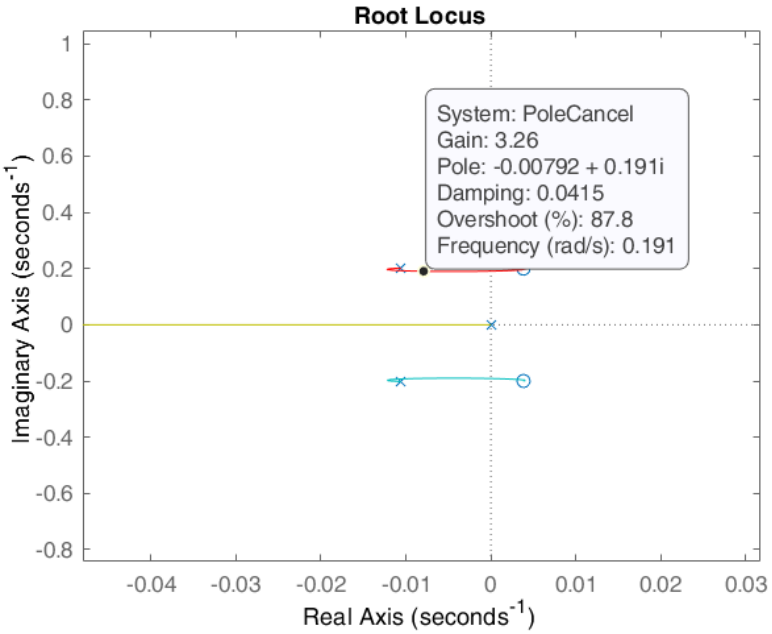

Figure 3: The root locus plot of the open-loop system

We use an integrator action to eliminate the steady-state error as this is a requirement. An integrator action will create oscillations and as our overshoot needs to be less then 1% we end up with a value of $K_i = 0.26$. We don't need a derivative action as our system is already stable with an overshoot smaller then 1% With this I-controller we get the following properties:

Table 1: Properties in time-domain

Time-domain	Values
Settling-time	83.7071 s
Overshoot	0.9190%
Steady-state error	0

The bode diagram with the phase and gain margins are shown in figure 4 and the step response is shown in figure 5. We see that the phase margin is greater then 70.9 degree which we calculated in question 1.2 and indeed our overshoot is less then 1%.

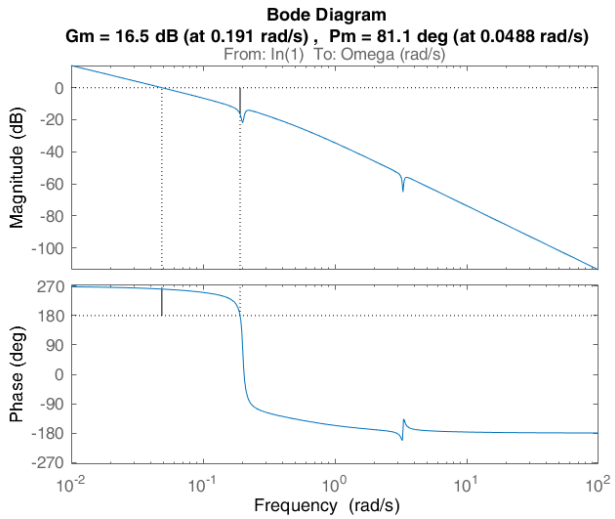

Figure 4: Bode diagram with margins of the open-loop system

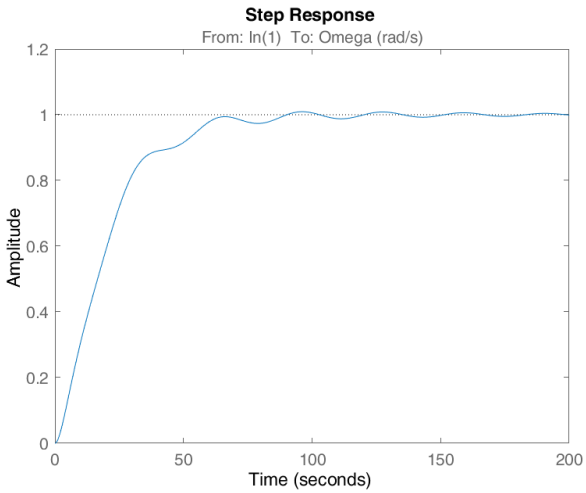

Figure 5: Step response of the closed-loop system

1.4

Here our reference tracking SISO controller is used to reject the output disturbance. The disturbance step input is applied on the third input channel of the state-space, a schematic overview can be seen in figure 6. Which results in the following step response in figure 7.

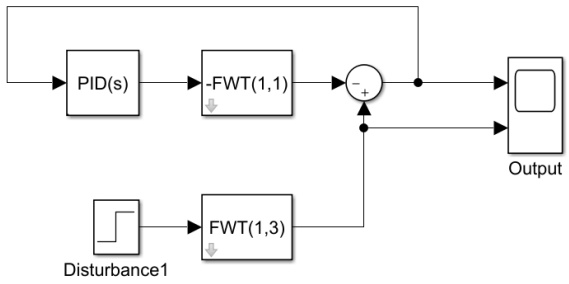

Figure 6: Overview of output disturbance rejection system

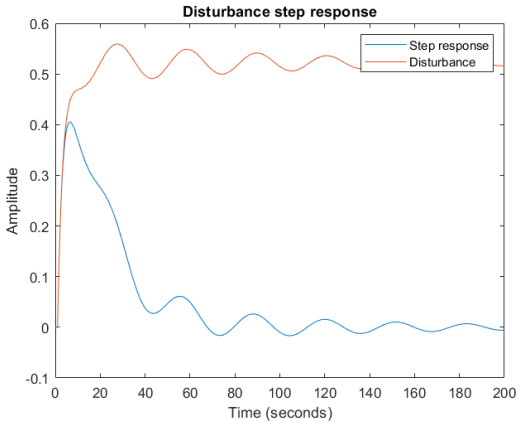

Figure 7: Step response of the closed-loop system with disturbance

The step response shows that the disturbance on the third input channel is well rejected as over time the controller goes to a steady state of zero. Therefore we wouldn't change our controller.

2 Multi variable Mixed-Sensitivity

2.1

To compute the Relative Gain Array (RGA) we apply the following formula.

$$RGA(G) = G \times \left(G^{-1}\right)^T \tag{4}$$

Where $\times$ resembles the element-wise product between matrices.
The RGA for $\omega = 0$ rad/s is:

$$\begin{bmatrix} -0.6554 & 1.6554 \\ 1.6554 & -0.6554 \end{bmatrix} \tag{5}$$

The RGA for $\omega = 0.6 * \pi$ rad/s is:

$$\begin{bmatrix} -0.0283 + 0.1398i & 1.0283 - 0.1398i \\ 1.0283 - 0.1398i & -0.0283 + 0.1398i \end{bmatrix} \tag{6}$$

Both RGA matrices by far don't resemble an identity matrix, therefore there is a lot of cross interaction between inputs and the outputs. Therefor applying a SISO system is not realistic and decoupling the system is very hard. Also it is interesting that the second RGA matrix is somewhat nearby the crossover frequency. As a RGA matrix resembling the identity matrix gives a stable system [2][p. 90]. However, that is clearly not the case.
Another thing that is interesting to point out is that for the steady state case the RGA matrix contains negative values on the diagonal. These input-output pairings should be avoided to obtain a stable plant [2][p. 90].

2.2

Table 2: Poles of MIMO system

Poles
$-0.0832 + 3.2936$i
$-0.0832 - 3.2936$i
$-0.4104 + 0.0000$i
$-0.0106 - 0.2022$i

Table 3: Zeros of MIMO system

Zeros
$-0.0078 + 1.2358$i
$-0.0078 - 1.2358$i

The two zeros are close to the origin and this can cause problems for uncertain plants. As the LHP-zeros may move to the RHP. Besides that the pole-zero locations don't further implement any limitations for our controller as the system is already quite stable because they are all in the LHP.

2.3

For w_{P11} we can use the formula:

$$w_{P11} = \frac{s/M_{11} + \omega_{B11}}{s + \omega_{B11} A_{11}} \tag{7}$$

with M_{11}=3 (desired bound on the H-infinity norm), ω_{B11}=0.3 Hz (cut-off frequency) and A_{11}=1/1000 (desired disturbance attenuation inside bandwidth). Filling the values into equation 7 gives us the following performance weight element.

$$w_{P11} = \frac{s/3 + 0.3 * 2 * pi}{s + 0.3 * 2 * pi * 10^{-4}} \tag{8}$$

2.4

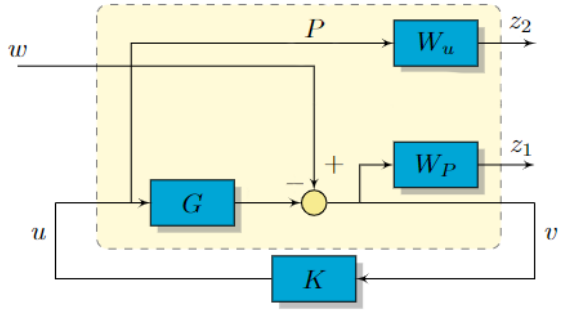

Figure 8: Block diagram of the model of the floating wind turbine and controller and include the performance weights W_p and W_u

2.5

For the generalized plant we have:

$$P = \left[\begin{array}{c|c} P_{11} & P_{12} \\ \hline P_{21} & P_{22} \end{array}\right] \tag{9}$$

With:

$$\begin{array}{ll} P_{11} = \begin{bmatrix} W_p \\ 0 \end{bmatrix} & P_{12} = \begin{bmatrix} -W_p G \\ W_u \end{bmatrix} \\ P_{21} = I & P_{22} = -G \end{array} \tag{10}$$

$$W_p = \begin{bmatrix} \frac{s/3+0.3*2*pi}{s+0.3*2*pi*10^{-4}} & 0 \\ 0 & 0.2 \end{bmatrix} \tag{11}$$

$$W_u = \begin{bmatrix} 0.01 & 0 \\ 0 & \frac{5\cdot10^{-3}s^2+7\cdot10^{-4}s+5\cdot10^{-5}}{s^2+14\cdot10^{-4}s+10^{-6}} \end{bmatrix} \tag{12}$$

$$\begin{bmatrix} z_1 \\ z_2 \\ v \end{bmatrix} = \begin{bmatrix} P_{11} & P_{12} \\ P_{21} & P_{22} \end{bmatrix} \begin{bmatrix} w \\ u \end{bmatrix} \tag{13}$$

The dimension of P is 6x4. These dimensions make sense as w consists of a the reference signal for ω_r and the disturbance from V. u contains the control inputs β and τ_e. This meets the number of columns for P. As u has dimension 2×1 the dimension of z_2 is the same. The output of the plant (v) contains ω_r and z, given this fact z_1 also has dimensions 2×1. Therefore also meeting the number of rows of P.

Using the functions 'augw' and 'minreal' in Matlab we find that the generalized plant has 8 states: ω, z_1, $\dot{z_1}$, z_2, $\dot{z_2}$, 2 states from Wu and 1 state from Wp.

2.6

The control design target is to make sure that the control input τ_e must have no steady state contribution. Meaning that a unit step change in the wind disturbance channel should still result in $\lim_{\tau_e \to \infty} = 0$.
Therefore we need to look at W_u as it implies weights boundaries on the behaviour of the control inputs. For the H_∞ mixed-sensitivity application it is required that $||N||_\infty < 1$ with

$$N = \begin{bmatrix} W_p S \\ W_u K S \end{bmatrix} \tag{14}$$

therefore $|KS| < 1/|W_u|$ must hold. So the desired behavior of the control inputs is bound by W_u.
W_u is defined in equation 12. Conform figure 8 this gives the following relation:

$$\begin{bmatrix} z_{21} \\ z_{22} \end{bmatrix} = \begin{bmatrix} 0.01 & 0 \\ 0 & \frac{5 \cdot 10^{-3} s^2 + 7 \cdot 10^{-4} s + 5 \cdot 10^{-5}}{s^2 + 14 \cdot 10^{-4} s + 10^{-6}} \end{bmatrix} \begin{bmatrix} \beta \\ \tau_e \end{bmatrix} \tag{15}$$

To analyze the bottom right element (Wu_{22}) it is plotted inversely in a magnitude plot.
As it consists of a matrix we will look at each element separately. First we analyze the behaviour of Wu_{22}. whose inverse shows he boundaries of the control sensitivity for the generator torque.

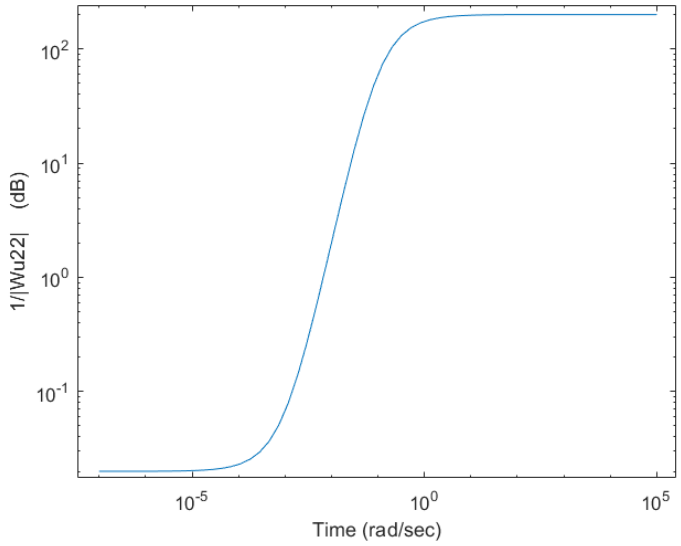

Figure 9: Magnitude plot of $1/Wu_{22}$.

As one can see it for low frequencies the control input τ_e is bounded close to zero. This is important as when t $\to \infty$ it means that $\omega \to 0$. So it shows almost no static contribution.

The upper left value (Wu_{11}) shows that the control input β is bounded by a constant value of 100 for all frequencies. But that is of no concern as our design requirement focuses on the other control input.

2.7

The generalized plant has 8 states as stated before. Two of which are caused by W_u and one is caused by W_p. This is because W_u has a second order term which contains 2 poles and thus 2 states and W_p has a first order term with one pole and so one state. The other 5 states are ω, z_1, $\dot{z_1}$, z_2 and $\dot{z_2}$. If we calculate the poles of the loop transfer function we see that we have two poles in the RHP. In table 4 the poles are shown.

Table 4: Poles loop transfer function

	Poles
1	$-57.2562 + 0.0000\text{i}$
2	$0.0221 + 3.5415\text{i}$
3	$0.0221 - 3.5415\text{i}$
4	$-0.0597 + 0.2136\text{i}$
5	$-0.0597 - 0.2136\text{i}$
6	$-0.0557 + 0.0631\text{i}$
7	$-0.0557 - 0.0631\text{i}$
8	$-0.0002 + 0.0000\text{i}$

According to the generalized (MIMO) Nyquist theorem [2][p. 152] the system is internally stable if and only if the Nyquist plot of det(I+L(s)) makes as many anti-clockwise encirclements of the origin as there are RHP poles and does not pass through the origin. If we look at the nyquist plot in figure 10 and at the zoomed-in one in figure 11 then we see that this is the case which indicates that our system is internally stable.

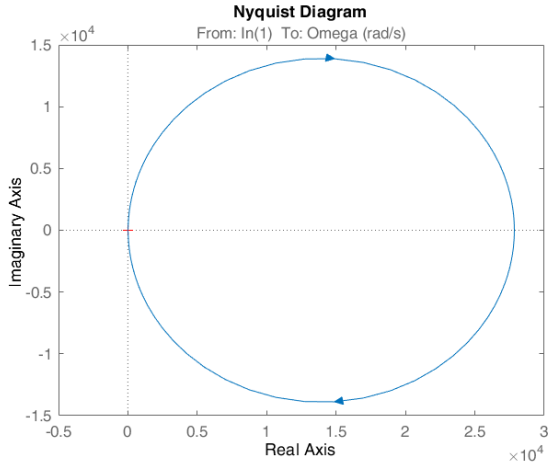

Figure 10: Nyquist

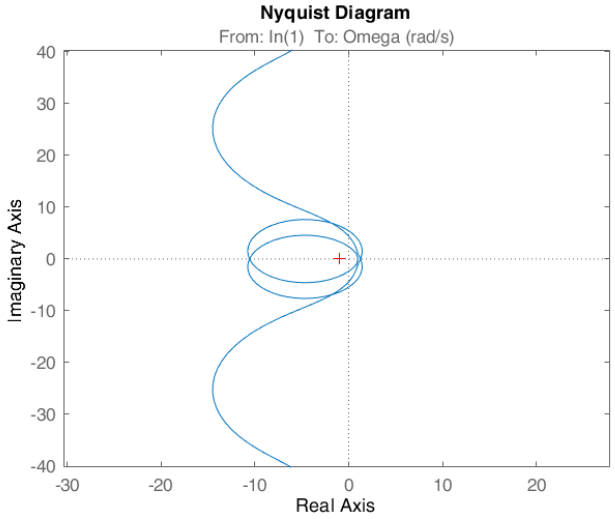

Figure 11: Zoomed-in Nyquist

2.8

To analyze the obtained system we take a look at the equation

$$y = (I + GK)^{-1}GKr + (I + GK)^{-1}G_d d \tag{16}$$

in which G is the plant, K the controller, G_d the disturbance gain, r the reference input and d the disturbance. Furthermore we see that the sensitivity ($(I + GK)^{-1}$) defines the influence of the disturbance on the output and the complementary sensitivity ($(I+GK)^{-1}GK$) the influence of the reference on the output. So to see how well our controller tracks the reference we use the complementary sensitivity and to see how well our controller rejects the disturbance we use the sensitivity times the disturbance gain (G_d). In this assignment the reference input is the rotational velocity ω_r. To see how well our controller tracks this reference we are plotting the step response of ω_r on ω_r and on the displacement z. In figure 12 we see that for a step on the reference the rotational velocity converges to 1 which means there is no steady-state offset. The settling time is around 10s and the overshoot is around 10%. The displacement converges to 1.5 for a step on the reference. This is a

quite significant steady-state offset as the unit of the displacement is meters. The settling time is 51s and the overshoot is 32% which is quite large as well.

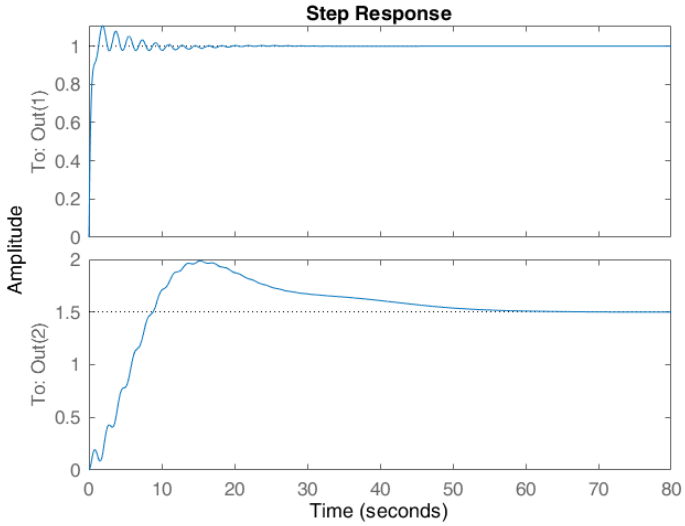

Figure 12: Step response on the rotational velocity

In this assignment the disturbance is the wind speed V and so we plot in figure 13 the step response of the wind speed on the rotational velocity ω_r and on the displacement z. In the figure we see that the disturbance is rejected quite well by the rotational velocity as the system converges fast to 0 so there is no steady-state error. There is a relatively high peak but it is damping quite fast. The settling time is 50s. For the displacement of the tower the disturbance is rejected much slower and with much oscillation and converges to around -0.2 which is the steady-state offset. Also the settling time (376s) is much higher than for the rotational velocity.

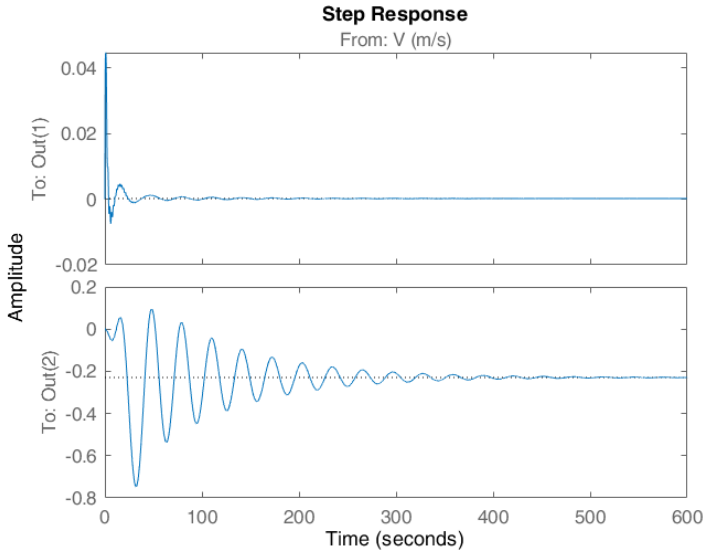

Figure 13: Step response of the disturbance

3 MIMO weighting design

3.1

In figure 14 we see a block diagram of the generalized plant.

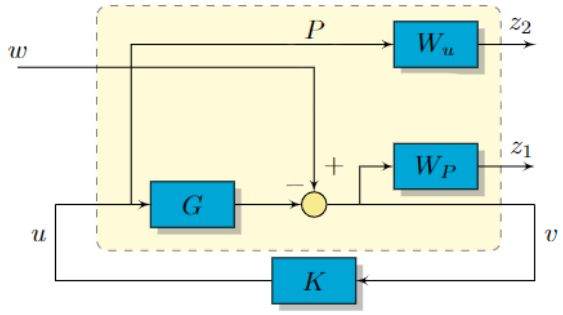

Figure 14: Block diagram of the model of the floating wind turbine and controller and include the performance weights W_p and W_u

We have one output, ω_r, that goes into the controller and two outputs, z_1 and z_2, that do not get into the controller. We have two control inputs, τ_e and β, and we have one disturbance input, wind speed (V). Signal w that goes in to the plant consists of a disturbance input (wind speed). The disturbance input is multiplied by the transfer function between input V to output ω_r. Our plant then has the following structure:

$$\begin{bmatrix} z_1 \\ z_2 \\ v \end{bmatrix} = \begin{bmatrix} W_p G_d & -W_p G_1 & -W_p G_2 \\ 0 & W u_{11} & 0 \\ 0 & 0 & W u_{22} \\ G_d & -G_1 & -G_2 \end{bmatrix} \begin{bmatrix} w \\ u_1 \\ u_2 \end{bmatrix} \tag{17}$$

G_d is the transferfunction of the disturbance to create the sine wave accompanied by the noise, G_1 is the transferfunction between the blade pitch (β) and the output ω_r and G_2 is the transferfunction between the generator torque (τ) and the output ω_r.

3.2

To achieve the best disturbance rejection we chose to make use of the following equation [2][p. 65]:

$$w_P(s) = \frac{\left(s/M^{1/2} + \omega_B^*\right)^2}{\left(s + \omega_B^* A^{1/2}\right)^2} \tag{18}$$

The value for M is obtained from the previous part and at first we also kept the cut-off frequency (ω_B^*) the same. But after performing some simulations the value of 0.6π radians seemed too strict for the system and we choose to lower it to 0.2π radians.

3.3

The weight W_u is a matrix with on the diagonal one weight component for β and one for τ. We want to choose this weight in such a way that β performs the control action for the low frequencies and τ for the high frequencies. We chose to apply two lead-lag filters for this design with the goal to have a relatively high gain in low frequencies and a low gain in high frequencies for β and a low gain in low frequencies and a high gain in high frequencies for τ. A lead-lag filter has the following form:

$$C(s) = k\frac{\tau_1 s + 1}{\tau_2 s + 1} \tag{19}$$

After iteratively trying several values for the lead-lag filter we choose the following controller weights for β and τ:

$$C_\beta = 0.1\frac{1000s + 1}{0.1s + 1} \tag{20}$$

$$C_\tau = 0.0001\frac{0.0001s + 1}{1000s + 1} \tag{21}$$

We plot the inverse of the controller weights to show the boundaries of our desired control sensitivity function in figure 15. We see in this figure that from a frequency of 0.1 rad/s the control action of the torque becomes dominant of the control action of the blade pitch.

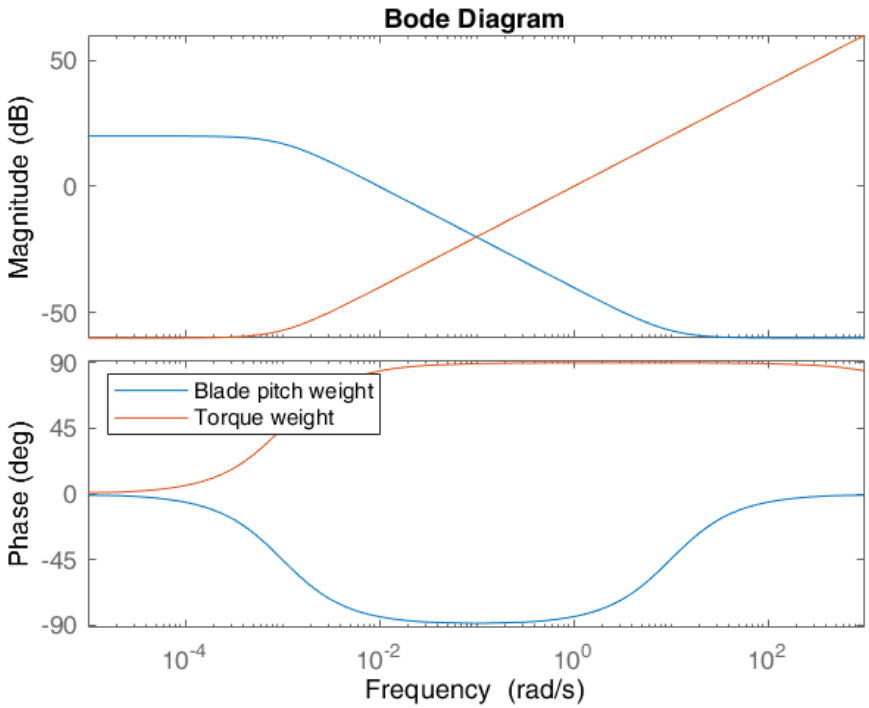

Figure 15: Bode plot of the inverse of the controller weights

3.4

As mentioned before in question 2.6 it is important that for the H-infinity norm all the values in equation 14 are smaller than 1. Therefore the desired bounds of the sensitivity and the control sensitivity are respectively limited by $1/|W_p|$ and $1/|W_u|$. In figure 16 the sensitivity of our system is plotted.

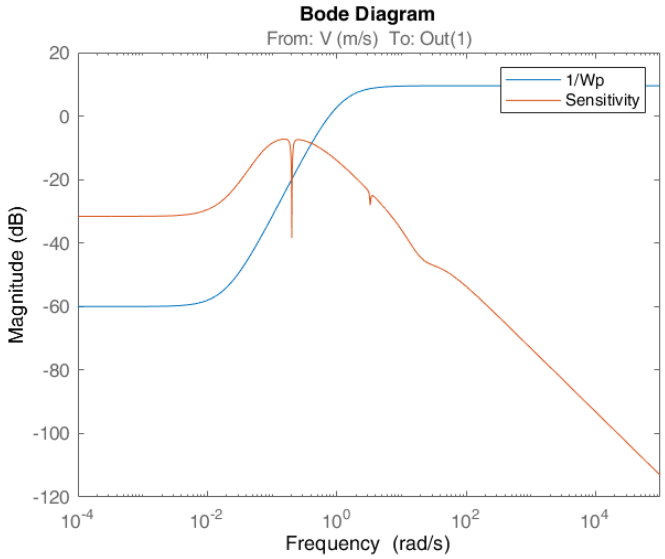

Figure 16: Bode plot of the inverse of the performance weights vs the sensitivity

The first thing that stands out from the above plot is the sensitivity at the lower frequencies, as it violates the specified bound. However, it doesn't seem like a significant problem for our system. As the sensitivity is at its highest peak around 0.1 and for all the other frequencies way below it. This can also be seen in a time plot of the sensitivity function which shows a small deviation in the system (see next section).

In the next two plots the controller weights of both control inputs are compared with their controller sensitivities.

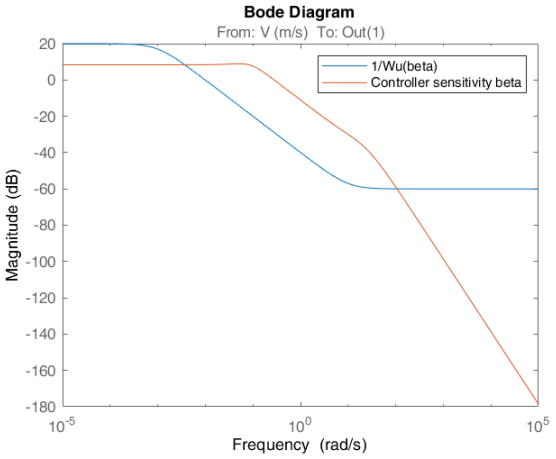

Figure 17: Controller weight of beta vs the controller sensitivity

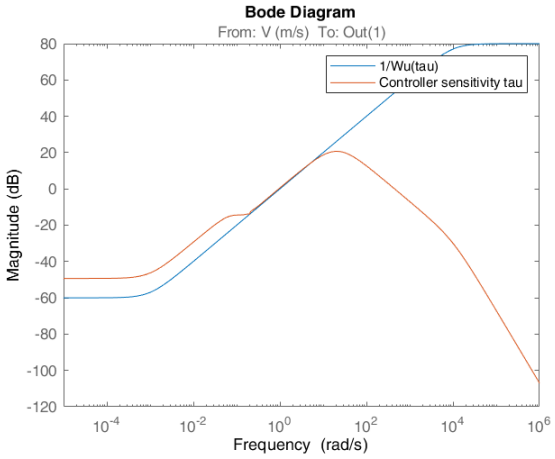

Figure 18: Controller weight of tau vs the controller sensitivity

Both sensitivity functions follow the desired behaviour of the control weights for most of the time. And the important design requirement, making sure the τ_e doesn't have a static contribution, seems to be met. Because although the controller sensitivity of τ_e is above the specified controller weight at the low frequencies it stays about max 10 dB above the controller weight. Which seems reasonably for the dB region in which it is happening.

3.5

In figure 19 and figure 20 we plotted the winddata versus the control action of both control inputs. The winddata has a lot of high frequency noise which we want to counter with the torque according to this assignment. In figure 19 we see that the line of β looks like a sinus function with a low frequency which means that it indeed counters the low frequency signals. In figure 20 we see that the torque has a lot of spikes and is horizontal which means that the torque is countering the high frequency noise of the wind. This means that our controller works good enough, but it could be better. If we would have an ideal controller, the plot of the control action of β would have been a smooth sinus. However, it is rather difficult to design a perfect controller as it is very hard to decouple the system as we saw in question 2.1.

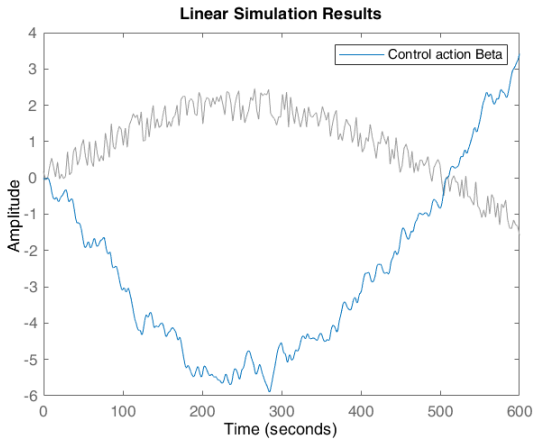

Figure 19: Controller action Beta vs Wind data

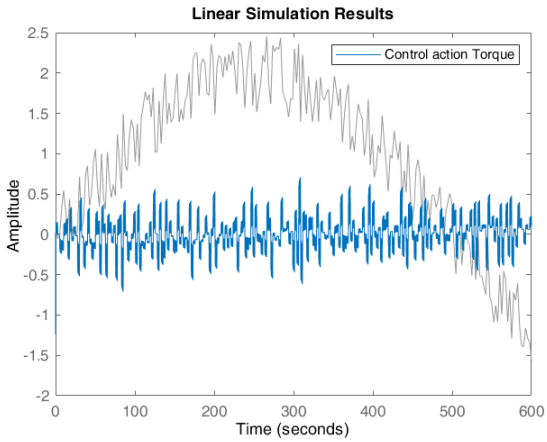

Figure 20: Controller action Torque vs Wind data

In figure 21 we see that there is a small error the whole time in the controller, but as mentioned before it is very hard to design a perfect controller in this situation.

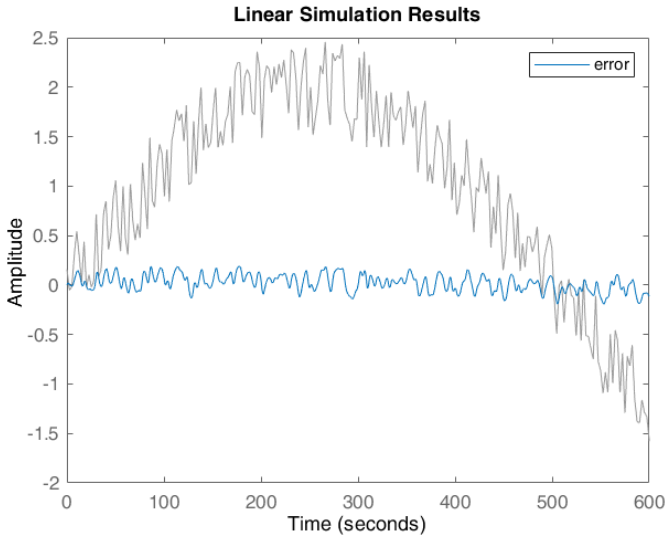

Figure 21: Controller error vs Wind data

We can also plot a noiseless sinus wave with a period of 1000s and see which control input reacts the most. We would aspect that β performs the control actions in this case as the input signal has a very low frequency. In figure 22 we see that there is also a small control error for a noiseless sinus input signal.

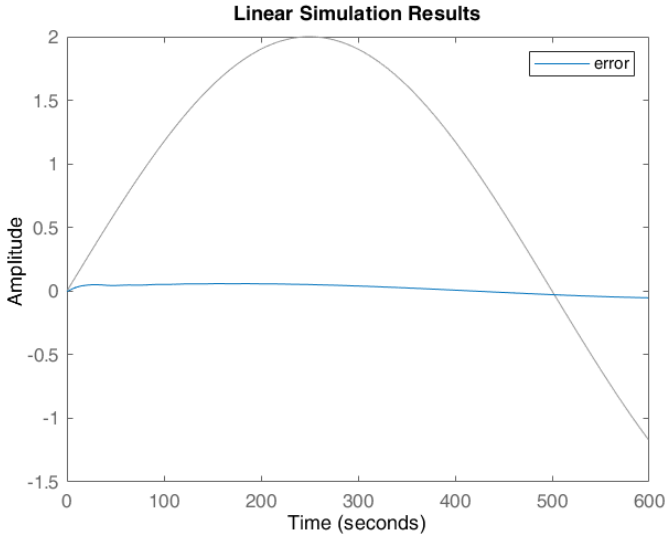

Figure 22: Controller error vs sinus

In figure 23 we see that β has a quite big control action which we expected and in figure 24 we see that τ_e has a very small control action. Again we see that our controller works, but that it could be improved. The controller could be improved by choosing different weights.

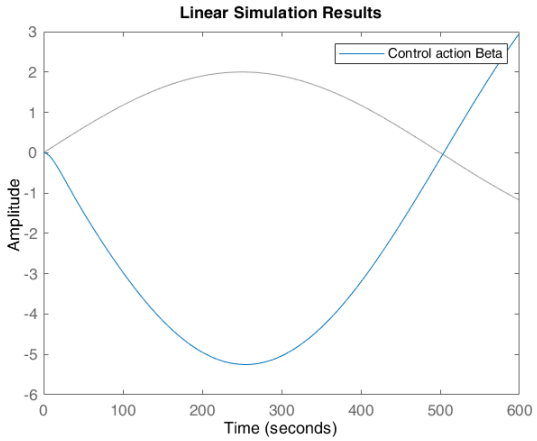

Figure 23: Controller action Beta vs sinus

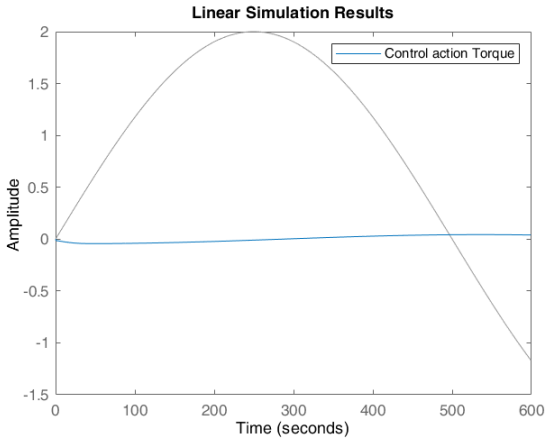

Figure 24: Controller action Torque vs sinus

References

Franklin, G., David Powell, G., & Emami-Naeini, A. (2019). *Feedback Control of Dynamic Systems, Global Edition* (8th ed.). Pearson.

Skogestad, S. (2005, 11). Multivariable Feedback Control: Analysis and Design. In (2nd ed.). Wiley-Interscience.